

# Film thickness measurement and contamination layer correction for quantitative XPS

J. Walton,<sup>a\*</sup> M. R. Alexander,<sup>b</sup> N. Fairley,<sup>c</sup> P. Roach<sup>d</sup> and A. G. Shard<sup>e</sup>

In order to determine the most appropriate method of measuring film thickness using imaging XPS, a series of thin polymer films have been prepared and analysed using spectroscopy. The thickness of these thin polymer films has been determined using peak shape analysis and by using photoelectron peak areas compared with a bulk reference and by using relative sensitivity factors. These results have been compared with values obtained using ellipsometry. The values obtained by measuring photoelectron peak areas were seen to be influenced by the chemistry of the film, so that a bulk reference of similar chemistry to the film is required for accurate thickness measurement. The values obtained using peak shape analysis, both interactive and non-interactive, were not dependent on the chemistry of the film and showed good agreement with ellipsometry. Imaging of a patterned polymer film was successfully carried out, and the polymer cross section was shown to provide a reasonable description of the inelastic background from the carbonaceous contamination layer. An image of the substrate photoelectron intensity was successfully corrected for attenuation in both the carbonaceous contamination layer and the polymer film simultaneously using an image of the film thickness determined by non-interactive peak shape analysis. This procedure is suitable for automated film thickness measurement and correction for attenuation in the carbonaceous contamination layer in both spectroscopy and imaging. Copyright © 2016 John Wiley & Sons, Ltd.

**Keywords:** XPS; imaging; film thickness; peak shape analysis; carbonaceous contamination

## Introduction

The surface sensitivity of X-ray photoelectron spectroscopy is a consequence of the low kinetic energy of the emitted electrons, and together with ease of quantification has resulted in its widespread use for the characterisation of surfaces. This surface sensitivity also lends itself to nano-structural characterisation and in particular to the measurement of film thickness. Many different procedures have been developed to measure film thickness using XPS which include sputter depth profiling, Angle Resolved XPS (ARXPS), attenuation of the photoelectron intensity in an overlayer, the relative intensity of chemically shifted peaks from the substrate and overlayer, and peak shape analysis which is dependent on changes in the intensity of inelastically scattered electrons.<sup>[1]</sup> Sputter depth profiling is not widely used in XPS because of the chemical state degradation caused by energetic monatomic ion beams, although the recent development of argon cluster sources is likely to see increased use for the analysis of polymeric materials. Each of these procedures has their own merits, but very often they require extra information such as the inelastic mean free path (IMFP), the Effective Attenuation Length (EAL), the intensity/energy transmission of the spectrometer, and an intensity reference, all of which may or may not be readily available. Furthermore some of these procedures are significantly affected by the environmental contamination layer present on all surfaces exposed to ambient. Recently X-ray photoelectron spectroscopic imaging, where a spectrum is acquired at each pixel in an image, either through scanning the sample or through full field imaging, has demonstrated the capability of producing quantified surface chemical state images.<sup>[2]</sup> It is therefore possible to apply the above procedures, to such spectroscopic image data sets in order to produce maps of film thickness, with the proviso that the procedures must be completely automated as

individual inspection of the large number of spectra contained in such data sets is not possible.

Examples of film thickness mapping have mostly used two different methods: the relative intensity of chemically shifted peaks from the overlayer and substrate, and the examination of inelastically scattered electrons. The first method has been used to measure the thickness of germanium oxide islands,<sup>[3]</sup> the thickness of buried silicon sub-oxide layers,<sup>[4]</sup> and the thickness of oxides on polycrystalline nickel.<sup>[5]</sup> The advantage of this procedure is that because the photoelectrons from the overlayer and substrate have similar energies the thickness measurement is not significantly affected by the presence of a contamination layer and the photoelectron region around only one element needs to be acquired. However this procedure does require estimation of the bulk intensity, which may be difficult to measure because of the presence of contamination, and also relies on the existence of a chemical shift between overlayer and substrate, and so is not generally applicable. The second method has been used to

\* Correspondence to: J. Walton, TSTC Ltd, 5 Grosvenor Terrace, Teignmouth TQ14 8NE, UK.  
E-mail: jrw2120@gmail.com

a TSTC Ltd, 5 Grosvenor Terrace, Teignmouth TQ14 8NE, UK

b School of Pharmacy, The University of Nottingham, Nottingham NG7 2RD, UK

c Casa Software Ltd, 5 Grosvenor Terrace, Teignmouth TQ14 8NE, UK

d Institute for Science and Technology in Medicine, Keele University, Keele ST5 5BG, UK

e National Physical Laboratory, Middlesex, TW11 0LW, UK

investigate patterned octadiene on a silver surface, plasma dissociated propanol on Teflon, and silicon dioxide on silicon.<sup>[6–9]</sup> Again the photoelectron region around only one element needs to be acquired, but it does require measuring the photoelectron intensity and inelastic background from a bulk sample, and may require determination of the intensity/energy transmission of the instrument.

It is also possible to determine the overlayer thickness by measuring the photoelectron intensity from the overlayer and comparing it to the intensity from the bulk under the same acquisition conditions. The necessity for a bulk reference can be eliminated by quantifying the data over all photoelectron regions but this procedure introduces uncertainty where an element has low concentration, particularly if it has a low sensitivity.

At this point it is worth mentioning ARXPS, where increasing the photoelectron emission angle makes XPS more surface sensitive allowing the thickness of the overlayer to be determined. This method requires a very flat surface which is the case here. However in the case of full field imaging tilting the sample by the required amount will move off axis regions out of the focal plane especially as the depth of field becomes smaller at higher spatial resolution. In the case of scanned probe imaging the shape of the analysis area will change from an oblong at normal incidence to a trapezoid at larger emission angles. It is likely that this added complexity will militate against widespread use of these techniques. The exception is where an instrument is capable of measuring the intensity of photoelectrons as a function of photoelectron emission angle without changing the sample orientation so that scanning the sample allows maps of film thickness to be produced.<sup>[10]</sup>

The purpose of this work is to assess the suitability of the aforementioned procedures applied to X-ray photoelectron spectroscopic images. To this end thin films of plasma polymerised hexane (ppHex) of different thickness have been produced and their thickness determined by photoelectron spectroscopy compared with values determined by ellipsometry. A polymer thin film was used because of its insensitivity to hydrocarbon contamination from exposure to the environment, because it has been shown that the IMFP of carbonaceous contamination is very similar to that of an average polymer.<sup>[11,12]</sup> Furthermore, once the thickness of the carbonaceous contamination has been determined it is relatively straightforward to correct photoelectron intensities from the substrate for attenuation in the overlayer. The procedures have then been applied to a spectroscopic image data set obtained from a patterned ppHex thin film. X-ray degradation indices of similar hydrocarbon polymers (XPS of Polymers Database, Surface Spectra, Manchester, UK) suggest that degradation of the ppHex films during analysis will not be significant for the acquisition conditions used.

### Film thickness measurement

A brief description of the methods used to determine the thickness of the ppHex thin films which can be applied to spectroscopic imaging is provided below.

### Exponential attenuation in the overlayer

The simplest method to determine the thickness of a homogenous overlayer is to compare the photoelectron intensity from the overlayer with the intensity from bulk material using the same measuring conditions. Assuming exponential attenuation in the

overlayer and uniform thickness, the thickness  $d$  of the overlayer is given by:

$$d = -L_o^o(E) \cos \theta \ln \left( 1 - I_o / I_o^\infty \right) \quad (1)$$

where  $I_o$  is the measured photoelectron intensity from the overlayer,  $I_o^\infty$  is the intensity from the bulk overlayer material,  $L_o^o(E)$  is the EAL of the overlayer photoelectrons in the overlayer, and  $\theta$  is the emission angle with respect to the surface normal. Similarly the film thickness can be calculated from the attenuation of the substrate intensity:

$$d = -L_s^o(E) \cos \theta \ln \left( I_s / I_s^\infty \right)$$

where  $L_s^o(E)$  is the EAL of the photoelectrons from the substrate in the overlayer,  $I_s$  is the measured photoelectron intensity from the substrate, and  $I_s^\infty$  is the intensity from the bulk substrate material. Knowing the EAL allows the overlayer thickness to be determined. Historically the difficulty with this procedure has been to ensure that the film and reference surfaces are free of environmental contamination, although the increased use of cluster ion sources should help in this respect.

An alternate method, which does not necessitate using a bulk reference intensity, is to simply replace the overlayer/bulk intensity ratio with the fractional concentration of the overlayer material. This requires measuring the photoelectron intensities of all elements present and calculating their atomic concentrations. However where elements exist in low concentrations, a substrate with thick overlayer, or thin overlayer for example, then errors propagate through the quantification because of the normalisation procedure, especially for elements with low sensitivity. This method is subsequently referred to as the overlayer attenuation (OA) method.

### Analysis of the inelastic background

Tougaard has shown that the shape of the inelastic background associated with a photoelectron peak can be used to determine the structure of material in the surface.<sup>[13]</sup>

The background is calculated by convoluting the spectrum with the differential inelastic cross section  $K(E, T)$ , which when multiplied by the energy dependency of the IMFP,  $\lambda(E)$ , is largely invariant with energy  $E$ , so that it becomes possible to define a universal cross section:

$$\lambda(E)K(E, T) = \frac{BT}{(C + T^2)^2} \quad (2)$$

where  $B = 3000 \text{ eV}^2$ ,  $C = 1643 \text{ eV}^2$ , and  $T$  is the energy above the photoelectron peak. For materials exhibiting sharp plasmon structure a three parameter universal cross section is required:

$$\lambda(T)K(E, T) = \frac{BT}{((C - T^2)^2 + DT^2)} \quad (3)$$

For polymers, the values of these parameters are  $B = 434 \text{ eV}^2$ ,  $C = 551 \text{ eV}^2$ , and  $D = 436 \text{ eV}^2$ . A specific case of surface structural analysis is that of a homogeneous overlayer where the technique can be used to measure the film thickness. The Quantitative Analysis of Surfaces by Electron Spectroscopy software (QUASES Tougaard ApS, Odense, Denmark) is used to perform the analysis. The IMFP may be estimated using the TPP-2M method<sup>[14]</sup> if the

density, atomic mass, band gap, and number of free electrons are known. Then once appropriate values for the emission angle and inelastic scattering cross section have been selected, the film thickness is interactively changed until the calculated background matches the measured background corrected for the intensity/energy response of the instrument. This procedure is referred to as the 'QUASES-Tougaard' method.

However this interactive approach is not suitable for spectroscopic imaging where the procedure must be applied to many spectra. Instead an automated procedure has been developed which assumes an exponential form for the depth distribution.<sup>[15,16]</sup> The amount of substance (AoS) within  $3\lambda$  is given by:

$$(AoS)_{3\lambda} = \frac{L + \lambda \cos \theta}{1 - e^{-(3\lambda \cos \theta + L)/(L \cos \theta)}} \cdot A_p \cdot \frac{C_H}{A_p^H} \cdot (1 - e^{-3\lambda L}) \quad (4)$$

where:

$$L = \frac{B_1}{B_0 - B_1} \cdot \lambda \cos \theta \quad (5)$$

and  $A_p$  is the photoelectron peak area, and  $B_1$  is the value of the  $B$  parameter required to make the background meet the spectrum 30 eV to higher binding energy than the photoelectron peak.  $A_p^H$  and  $B_0$  are equivalent values for a homogeneous bulk reference, and  $C_H$  is the atom density ( $\text{nm}^{-3}$ ). The equivalent overlayer thickness  $d(\text{nm})$  is now defined as:

$$d = \frac{(AoS)_{3\lambda}}{C_H} \quad (6)$$

Because a bulk reference has been used there is no need to apply a correction for the intensity/energy response of the instrument. The procedure has been validated for thin films of gold buried at various depths in nickel.<sup>[17]</sup> This is referred to as the 'Tougaard Non-interactive' method.

### Attenuation lengths and IMFPs

All the procedures for film thickness measurement so far described rely on the accurate determination of the IMFP or EAL. The EAL should be used where elastic scattering is important and where the film thickness is determined solely by the photoelectron intensity.<sup>[18]</sup> Where the thickness is determined by peak shape analysis the IMFP is usually used. It has been shown that for thin layers of gold in nickel the effect of elastic scattering is less than 10% for depths less than 1.5 IMFP and increases to 25% for 2.5 IMFP.<sup>[19]</sup> For less dense materials the effect of elastic scattering will be less important and so the IMFP has been used in this work for the determination of the thickness of polymeric material using peak shape analysis. The TPP-2M calculation results in an IMFP of 3.0 nm for C 1s photoelectrons in carbon, generated by Al K $\alpha$  X-rays. Seah and Spencer<sup>[20]</sup> reported values of 3.1 nm and 3.5 nm for glassy carbon and polymeric carbon respectively. Seah has since developed a simple universal curve for the energy dependency of both the IMFP( $\lambda$ )<sup>[21]</sup> and EAL( $L$ )<sup>[22]</sup> which may be used in the absence of more accurate measurements as:

$$\lambda = (0.73 + 0.0095E^{0.872})/Z^{0.3} \quad (\text{nm}) \quad (7)$$

$$L = (0.65 + 0.007E^{0.93})/Z^{0.38} \quad (\text{nm}) \quad (8)$$

where  $E$  is the photoelectron kinetic energy and  $Z$  is the average atomic number. These equations result in an IMFP of 3.5 nm and

EAL of 3.4 nm for C 1s photoelectrons excited by Al K $\alpha$  X-rays, in a polymer hydrocarbon using an average atomic number of 4. The accuracy of the universal equations are estimated at 11.5% and 9% for the IMFP and EAL respectively. In the following determination of polymer film thickness, values of the IMFP and EAL have been calculated using the universal equations because these produced thickness values closest to those measured by ellipsometry, did not result in unexpectedly large elastic scattering, and allow a consistent method to calculate ALs for photoelectrons of different energy to enable their intensity to be corrected for attenuation in an overlayer.

### Experimental details

Thin films of ppHex deposited on clean fused silica have been analysed using ellipsometry, atomic force microscopy, and XPS in order to assess the merits of different photoelectron spectroscopic procedures in measuring film thickness. These procedures have then been applied to a photoelectron spectroscopic image data set acquired from a patterned ppHex film to produce maps of film thickness.

### ppHex deposition

Thin films of ppHex were deposited onto fused silica disks (UQG Optics, Cambridge, UK) in a purpose built plasma reactor, which has been described previously.<sup>[23]</sup> The samples were electrosonically cleaned in analar ethanol and then exposed to UV ozone for 20 min before insertion into the reactor. They were further cleaned by exposure to an oxygen plasma for 3 min before deposition of the ppHex thin films. The ppHex films were deposited at a pressure of 0.44 mbar and 20 W power, and the nominal film thickness was monitored *in situ* by a quartz crystal microbalance (QCM). Films of nominal thickness 0.58, 1.10, 2.13, 2.17, 4.03, 7.60, 10.05, and 19.91 nm as measured by the QCM were prepared. Two samples were made for each thickness and were then analysed by ellipsometry, AFM, and XPS.

The patterned ppHex films were made by first creating a holey photoresist film on the fused silica substrate through which ppHex was deposited. The photoresist film was then removed to leave islands of ppHex on the silica surface.

### Atomic force microscopy

Topographic analysis of the ppHex films was carried out using a Dimension 3100 atomic force microscope (Bruker Nano Surface, Santa Barbara, USA) operating in tapping mode, using TESPA probes with a nominal spring constant of 20 to 80 N/m and tip radius of 8 nm. Images of 512 × 512 pixels were acquired at various scan sizes up to 20  $\mu\text{m}$ , and analysed using Nanoanalysis software version 1.5.

### Ellipsometry

Film thickness determination by ellipsometry was carried out at the National Physical Laboratory, Teddington, UK using a M2000-DI spectroscopic ellipsometer (Woollam, Lincoln, Nebraska, USA). Ellipsometric data were acquired in the wavelength range 190 nm to 1700 nm at 50°, 55°, and 60° incidence angles, close to the Brewster angle of silica (~55.5°). Data were fitted using Woollam software WVASE32. A substrate-overlayer model was used in which both the substrate and overlayer were assumed to be optically isotropic. The optical constants of the silica substrate were obtained from a Sellmeier model provided in the software. The

overlayer could be modelled as a transparent film above 400 nm with a dispersion in refractive index following the Cauchy relationship  $n = \alpha + \beta w^{-2} + \gamma w^{-4}$ , where  $w$  is the wavelength of light. Fitting to the thickest film gave a best fit mean square error of 1.3, with a thickness of 38.9 nm,  $\alpha = 1.492$ ,  $\beta = 0.00486 \mu\text{m}^2$  and  $\gamma = 0.00018 \mu\text{m}^4$ . The optical constants derived in this manner were retained in the model to fit data from thinner films to obtain film thicknesses relative to the thickest film. Because of the assumptions used here and the correlation between thickness and refractive index for thin films, the relative accuracy of ellipsometric thickness reported here are approximately 10%. For thicker organic films, approximately 100 nm, the relative accuracy of this method compared to traceable XRR measurements is approximately 4%.<sup>[24]</sup>

## XPS

X-ray photoelectron spectroscopic analysis was carried out using a Kratos Axis Ultra DLD at the University of Manchester. The spectra were generated using monochromatic Al K $\alpha$  radiation ( $h\nu = 1486.6 \text{ eV}$ ) at 300 W power and images using 150 W, with a base pressure  $1.0 \times 10^{-9}$  mbar, and charge neutralisation achieved by low energy electrons produced by passing a current of 1.8 A through an elliptical filament located at the lower end of the electrostatic lens. Wide scan spectra for sample characterisation were acquired from 1100-eV to 0-eV binding energy, using hybrid lens mode which utilises both magnetic and electrostatic lenses, at 80-eV pass energy, and 0.8-eV step size. This results in an energy resolution of 1.4 eV for the Ag 3d<sub>5/2</sub> photoelectron peak. For film thickness measurement the electrostatic lens mode was used to restrict the acceptance angle, and data was acquired from 650 eV to 0 eV binding energy, at 0°, 25°, 40°, 50°, 60°, and 70° takeoff angles after calibration of the surface normal using the crystal axis method.<sup>[25]</sup> In this case energy resolution was 1.8 eV for the Ag 3d<sub>5/2</sub> photoelectron peak. The spectroscopic image data was acquired at field of view 1, 800  $\mu\text{m} \times 800 \mu\text{m}$ , 80-eV pass energy, and 300-s dwell time per image, for the O 1s region from 580 eV to 490 eV, for the C 1s region from 330 eV to 240 eV and for the Si 2p region from 150-eV to 80-eV binding energy with a 1-eV step. Energy resolution for imaging was 2.2 eV for the Ag 3d<sub>5/2</sub> photoelectron peak. Principal component analysis was used to improve the signal/noise in the spectroscopic image data set prior to film thickness measurements. The data was quantified by measuring photoelectron peak areas and using theoretical sensitivity factors,<sup>[26]</sup> modified for the instrument geometry and the IMFP energy dependency.<sup>[27]</sup> The intensity/energy response of the instrument was determined following acquisition of spectra from clean copper, silver, and gold.<sup>[28]</sup> Charge referencing was made by reference to the hydrocarbon peak at 285.0 eV. All data processing was carried out using CasaXPS version 2.3.17dev6.4u (Casa Software Ltd, Teignmouth, UK).

## Results and discussion

### Characterisation of the fused silica substrate and ppHex films

The effectiveness of the cleaning procedure on the fused silica surfaces prior to deposition of the ppHex films was determined using XPS. Quantification of the wide scan spectra showed that the carbon concentration had been reduced from 20.2% on the as received surface to 7.9% following U.V. ozone cleaning. The carbon concentration prior to ppHex deposition is likely to be even lower

than this because an oxygen plasma was used to further clean the substrates once they were in the reactor. The surface elemental concentrations on the clean surface were O 58.8%, Si 32.6%, C 7.9% Na 0.2%, Ca 0.2%, and N 0.3%. The morphology of the fused silica surface was measured by AFM. The roughness average,  $R_a$ , measured over a 20  $\mu\text{m} \times 20 \mu\text{m}$  scan was 0.65 nm.

Once the ppHex films had been deposited ARXPS and AFM were used to detect any non-uniform film growth. In most cases a linear relationship was observed between  $\ln(1 - C_{\text{conc}})$  and the inverse of the cosine of the emission angle. All films showing non-uniform film growth were excluded from determination of the film thickness. The roughness average of the ppHex films used for thickness measurement determined by AFM was between 0.62 nm and 0.87 nm.

### Film thickness measurement

Results of the film thickness measurements obtained using all the different procedures are shown in Table 1.

### Comparison of QUASES-Tougaard method with ellipsometry

The film thickness has been determined from the inelastic background using Quases-Tougaard following correction of the spectra for the intensity/energy response of the spectrometer. A comparison of the film thickness values obtained by Quases-Tougaard and ellipsometry is shown in Fig. 1. The slope of 0.97 and intercept at the origin of 0.04 was determined using the first six points and shows very good agreement between the two techniques up to 16 nm. The correlation broke down only for the 30-nm-thick film,

**Table 1.** Thickness (nm) of ppHex films determined by different methods

Sample number	QCM	Ellipsometry	QUASES-Tougaard	Tougaard non-interactive	OAM—RSF	OAM—Ref
1	0.6	1.6	1.4	1.5	0.7	1.0
2	1.1	2.5	2.8	2.4	1.2	1.7
3	2.1	5.2	4.8	5.2	2.7	3.4
4	2.2	6.0	6.5	6.0	3.8	4.1
5	4.0	8.6	7.8	9.1	5.8	7.2
6	7.6	15.4	15.1	14.9	10.9	14.6
7	10.1	29.9	24.2	17.1	15.7	14.0

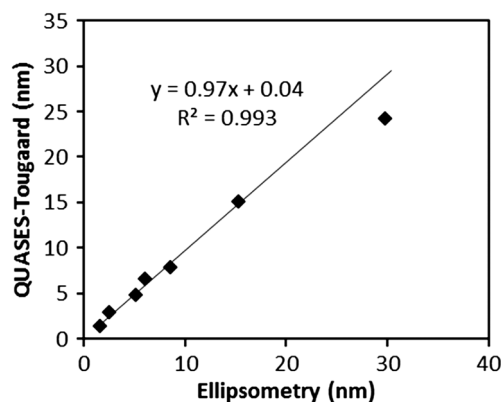


**Figure 1.** Comparison of film thickness measurements using ellipsometry and QUASES-Tougaard.



where the QUADES-Tougaard method underestimated the film thickness. This is not surprising because the film thickness is equal to  $7.8 \times \text{IMFP}$ . This comparison of film thickness measurement is comfortably within the estimated accuracies of ellipsometry and IMFP determination. Comparison with the QCM data showed that the QCM film thickness was underestimated by a factor of two. This discrepancy arises because of inhomogeneity in the plasma caused by electrical interaction with the QCM, the positioning of the QCM with respect to the samples, and the accuracy of estimation of the density of the deposited film in order to convert mass per unit area to thickness.

### Comparison of the Tougaard non-interactive method with ellipsometry

However, QUADES-Tougaard is an interactive procedure and so unsuitable for spectroscopic imaging where there are too many spectra to be individually examined. Instead Tougaard proposed an exponential approximation to the estimation of film thickness, where the AoS in the top few atomic layers could be calculated non-interactively, allowing an estimation of the film thickness to be made. The procedure involves measuring the photoelectron peak area using a linear background, and determining the value of the  $B_i$  parameter required to ensure that the background meets the spectrum 30 eV to higher binding energy than the photoelectron peak, when appropriate values for the other parameters describing the inelastic scattering cross section have been selected. The  $B_0$  value was determined from the nominal 20-nm-thick film, measured by ellipsometry as 38.9 nm, and the values used in Eqns (4), (5), and (6) to determine the film thickness. However if the universal cross section, Eqn (2), is used together with a value for the  $C$  parameter of 1643, then the background must be extended to 55 eV above the photoelectron peak in order to prevent the background cutting through the spectrum, which is more significant for the thicker films. In CasaXPS this is described as the 'U 2 Tougaard' background; the two parameter Tougaard background. The lower limit for the background was set at 270 eV. This procedure does not require correcting the data and reference for the instrument transmission, as spectra from the thin films and bulk material are equally affected. By using the polymer inelastic scattering cross section, Eqn (3), instead of the universal cross section, with  $C = 551 \text{ eV}^2$  and  $D = 436 \text{ eV}^2$ , the upper limit of the background can now be set to 315 eV, 30 eV to higher binding energy than the photoelectron peak, without the background cutting through the spectrum. In CasaXPS this is described as the 'U 3 Tougaard' background. This corresponds to the Tougaard three parameter cross section, with the default values set to those appropriate for a polymer. Figure 2 shows a comparison of the Tougaard non-interactive backgrounds for the C 1s photoelectron region produced using both the universal and polymer cross sections. Figure 3 shows a comparison of the ppHex film thickness measured using both cross sections with the thickness measured using ellipsometry. Both data sets can be fitted with a linear trend but the slope using the polymer cross section with ellipsometry is 0.98, whereas that using the universal cross section is 0.78. The polymer cross section also displays a smaller intercept, 0.06, at the origin. The use of the correct inelastic scattering cross section makes a considerable difference to the accuracy of film thickness measurement, and is valid to a thickness of 16 nm. Again, using the polymer cross section, the comparison of film thickness measurement falls within the estimated accuracy of ellipsometry and IMFP determination.

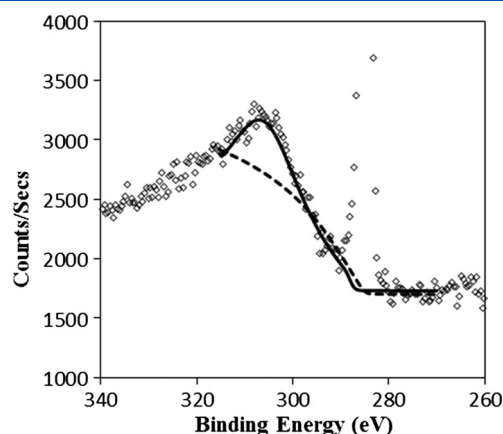


**Figure 2.** Expanded view of the C 1s photoelectron region showing the Tougaard non-interactive backgrounds using the universal cross section (dashed line) and the polymer cross section (solid line) from 315-eV to 270-eV binding energy.

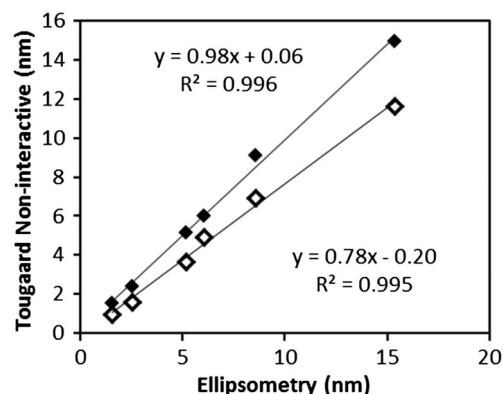


**Figure 3.** Comparison of film thickness measured using the Tougaard non-interactive method with a universal cross section (open symbols) and with a polymer cross section (filled symbols), and that measured using ellipsometry.

### Comparison of the OA method with ellipsometry

The film thickness was also calculated by measuring the C 1s photoelectron peak areas, and comparing these with the value obtained from a bulk reference, in this case the film measured at 38.9 nm thick by ellipsometry, using Eqn (1). An alternative to using a bulk reference material is to simply quantify the intensities using relative sensitivity factors and a normalisation procedure. The film thickness is then calculated in a similar way, but using the fractional concentration. The film thickness measured using both methods is compared with the thickness measured using ellipsometry and is shown in Fig. 4. A linear trend has been drawn through both sets of data, and shows a gradient of 1.0 for the thicknesses determined using a reference and 0.75 using relative sensitivity factors. However both show significant intercepts at the origin. There are significant differences in the measured thickness for the two thicker films.

The thickness calculated by the quantification method produces smaller values than those produced using a bulk reference. This difference is believed to be because of increased errors measuring low substrate intensities from thicker films, particularly where the relative sensitivity factor is small so that increased errors are incorporated through the normalisation step in the quantification procedure.

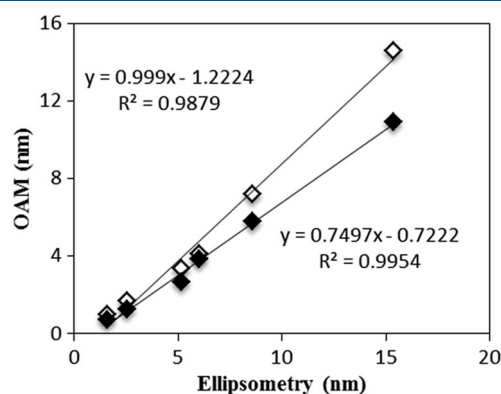


**Figure 4.** Comparison of the film thickness calculated using the overlayer attenuation method using a bulk reference (open symbols) and by quantification (filled symbols) with that measured using ellipsometry.

The thickness calculated by both methods for films between 3 nm and 7 nm show lower values than expected. This cannot be explained by the roughness of the fused silica substrate because the increased path length through an overlayer of even thickness would result in an over estimation of the film thickness. One possible explanation is that the ppHex films have uneven thickness, which is more significant for the thinner films than the thick films. Figure 5 shows an AFM height image over a  $4\ \mu\text{m} \times 4\ \mu\text{m}$  scan size, from the ppHex film measured as 8.59 nm by ellipsometry. Two types of features can be seen; a few relatively deep pits up to 4 nm, and a smaller undulating intensity of  $\pm 1\ \text{nm}$  over the entire surface. Because no deep pits like this were observed on the fused silica substrate it is reasonable to assume that these pits occur in

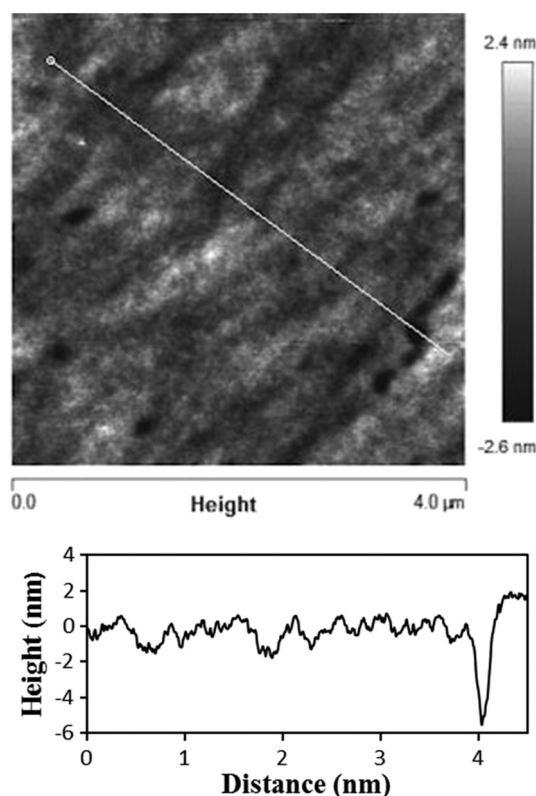


**Figure 5.** AFM height image ( $4\ \mu\text{m} \times 4\ \mu\text{m}$ ) from the ppHex film, measured as 8.59 nm by ellipsometry.

the ppHex film. The deep pit in the lower right of the image shows a peak to trough angle of only  $1.6^\circ$  and so would not be detected by ARXPS. However, bearing analysis shows that only 1.83% of the surface area is below 1.5 nm from the mean, and that only 0.67% is below 2 nm, which is not large enough to explain the deviation in measured film thickness. If the undulating thickness is assumed to be step like with a variation of  $\pm 1\ \text{nm}$  from the mean, then using an EAL of 3.41 nm results in a correction to the mean of 1.04, which would result in larger rather than smaller estimates of the film thickness. The discrepancy observed in the thickness measured by QUASES-Tougaard and the OA method cannot therefore be explained by film morphology.

Closer inspection of the C 1s photoelectron spectra from these films revealed the presence of components at 2.2 eV and 4.2 eV higher binding energy, which have larger relative intensity for the thinner films, and presumably arise from the presence of oxygen remaining from the plasma cleaning procedure prior to ppHex deposition. Although peak fitting to data acquired at 80-eV pass energy is not ideal, it was used to enable a correction to the C 1s photoelectron intensity to be calculated assuming that these components represented carbon bonded to one and two oxygen atoms respectively. The comparison between the film thickness calculated using the OA method with a bulk reference, corrected for the presence of oxygen, with ellipsometry has been replotted in Fig. 6, and shows a slope of 0.99. This suggests that oxidation, by causing a reduction in the number density of carbon atoms, is responsible for the lower film thickness measurement using the OA method. This is consistent with the fact that ellipsometry measures film thickness and is not sensitive to chemistry. The OA method by quantification is measuring relative to pure carbon, and in this case the OA method using a bulk reference is measuring relative to ppHex. Accurate determination of the film thickness by the OA method therefore requires use of a bulk reference of similar chemistry to the film being measured. Where the thickness of the carbonaceous overlayer is automatically determined and corrected,<sup>[29]</sup> then the Tougaard non-interactive procedure is the better option as it does not require a chemically similar bulk reference.

### Mapping film thickness

Mapping film thickness requires acquisition of spectroscopic image data sets, which can be converted to spectra at every pixel and then processed as described above for spectroscopy. First the spectroscopic image data was denoised using principal component analysis to reconstruct the data using the first four image components

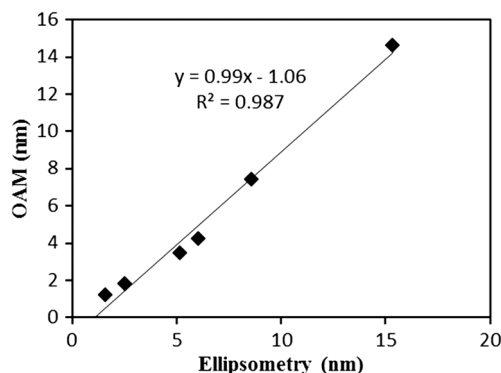


**Figure 6.** Comparison of the film thickness calculated using the overlayer attenuation method using a bulk reference following correction for oxygen in the ppHex film, with that measured using ellipsometry.

following root mean scaling in the spectral domain. The C 1s images were then converted to spectra. Maps of film thickness were calculated using the Tougaard non-interactive method and the OA method using a bulk reference and by quantification.

### Tougaard non-interactive method

First the  $B_1$  values at every pixel were calculated by fitting the C 1s inelastic background using the Tougaard three parameter cross section with  $C$  and  $D$  values of  $551 \text{ eV}^2$  and  $436 \text{ eV}^2$  respectively. The  $B_0$  value of  $501.1 \text{ eV}^2$  was determined from the nominally 20-nm-thick film, measured as 38.9 nm by ellipsometry. A scaling factor was calculated by comparing the C 1s area intensity measured in electrostatic mode with that from a single pixel at  $800\text{-}\mu\text{m}$  field of view. The scaling factor was then multiplied by the photoelectron peak area from the bulk in electrostatic mode to produce a bulk area value at a single pixel. The film thickness at every pixel was then calculated using Eqns (4), (5), and (6). In CasaXPS this requires selecting a background type labelled 'U 3 Tougaard' and tag field 'texp  $B_0 A \lambda \theta$ ' in the spectral quantification window, where  $B_0$  is the bulk  $B$  value,  $A$  is the bulk photoelectron peak area at a single pixel,  $\lambda$  is the IMFP of carbon photoelectrons in the ppHex, and  $\theta$  is the emission angle. These parameters are then propagated to all the spectra in the data set and a film thickness map produced by selecting the 'convert regions to images' operation in the image processing window. The map of film thickness is then normalised using the sum of all the photoelectron images divided by the mean, to take account of changes in X-ray flux across the field of view. The thickness map calculated this way is shown in Fig. 7 together with a cross section along the indicated line, which reveals approximately 4.0-nm-thick ppHex islands and 2.0 nm of contamination on the fused silica substrate.

A bright spot can be seen in the lower left corner of the thickness map, which inspection of the spectra from this location reveals to

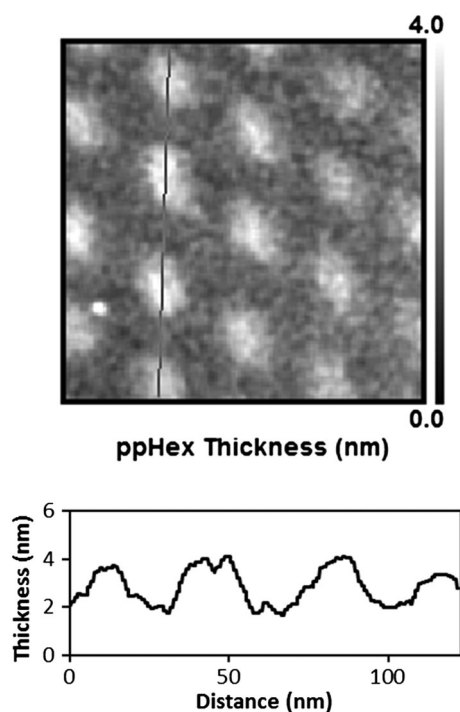


**Figure 7.** Image ( $800\text{ }\mu\text{m} \times 800\text{ }\mu\text{m}$ ) and cross section of the ppHex film thickness calculated using the Tougaard non-interactive method.

be rich in oxygen and depleted in carbon and silicon compared with the surrounding region. It is believed to be because of the presence of a contaminant particle. The particle appears bright because whilst the C 1s photoelectron intensity decreases the background arising from lower binding energy components remains high. Such particles do not comply with the assumption that the film is homogeneous.

In order to exclude the possibility that the inelastic cross section used was not appropriate for the carbonaceous contamination on the fused silica, regions were defined on the silica surface excluding areas of ppHex islands and the spectra from these regions summed. A background was fitted to the summed spectrum calculated using the three parameter polymer cross section to fit the data between 315-eV and 270-eV binding energy, and is shown in Fig. 8. This demonstrates that the polymer inelastic scattering cross section is suitable for use with a carbonaceous contamination layer. Because it has already been shown that the IMFP of carbonaceous contamination is similar to an average polymer, then this procedure may be used to determine the thickness of a contamination overlayer. Furthermore a hydrocarbon polymer may be used as a bulk reference for the carbonaceous contamination without concern that it may be contaminated.

### OA method

The same spectra used in the Tougaard non-interactive method above were used to measure the C 1s photoelectron peak area at every pixel using a linear background, which was then divided by the same bulk photoelectron peak area at a single pixel, as used above. This intensity ratio was then used in Eqn (1) to produce a map of film thickness, which is shown in Fig. 9. The silicon, oxygen, and carbon photoelectron peak areas were also used to quantify the spectra at every pixel, by correcting for the instrument response in imaging mode and using Scofield relative sensitivity factors modified for the geometry of the instrument and the IMFP energy dependency. The C 1s atomic concentration image was divided by 100 to produce a fractional concentration image which was then used in Eqn (1) to produce a map of carbon film thickness. The film thickness maps produced by the two OA methods, using a bulk reference and by quantification were almost identical, the quantification method showing ppHex islands approximately 2% higher. However, whilst the thickness pattern

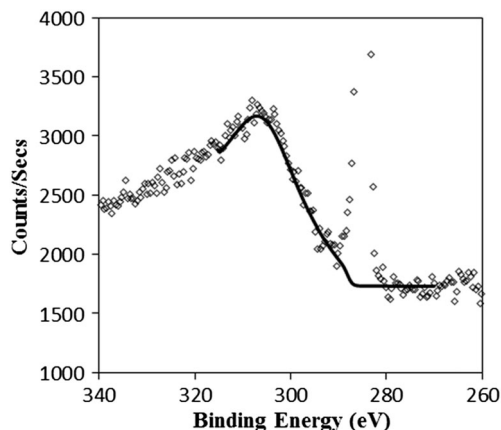


**Figure 8.** Tougaard non-interactive background using the polymer cross section fitted to the summed spectra from regions on the fused silica surface excluding the ppHex islands.



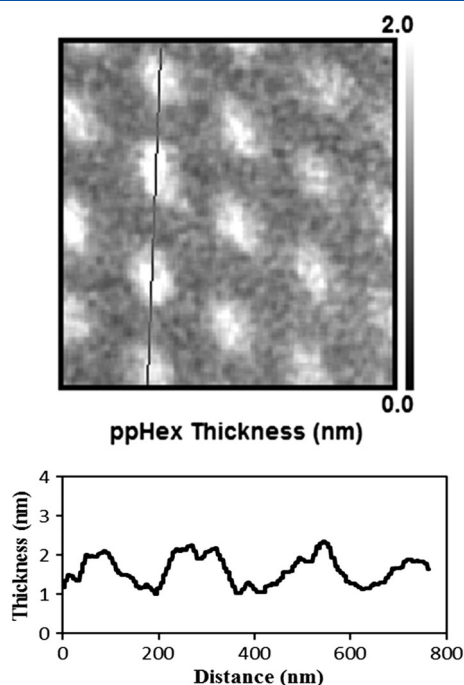


**Figure 9.** Image (800  $\mu\text{m} \times 800 \mu\text{m}$ ) and cross section of the ppHex film thickness calculated using the OAM with bulk reference.

produced by the OA method was similar to that produced by the Tougaard non-interactive method, the thickness scale was approximately 60% of that produced using the Tougaard non-interactive method. This is consistent with the differences observed in spectroscopy where the thickness of the four thinnest films determined by OA were a factor of 0.63 of the thickness obtained using QUASES-Tougaard.

By overlaying the thickness maps of Figs 7 and 9, the bright spot observed in the lower left corner of Fig. 7 is now seen as a slight reduction in film thickness, consistent with the observed decrease in C 1s photoelectron intensity. The interpretation of photoelectron intensities from this region is complicated by geometric effects from the contaminant particle which is approximately 40- $\mu\text{m}$  diameter.

### Correction of the substrate image for attenuation in the ppHex overlayer

Imaging XPS offers the possibility of comparing surface elemental and chemical state concentrations at different locations within the field of view. However this is complicated by the presence of the contamination overlayer which attenuates photoelectrons of different kinetic energy by different amounts and may not be evenly spread across the surface. Once a map of the overlayer thickness has been produced it is possible to correct the substrate intensities for attenuation in the overlayer, where the unattenuated substrate intensity  $I_s$  is given by:

$$I_s = I_s^m \times e^{(d/\lambda)}$$

where  $I_s^m$  is the measured substrate intensity,  $d$  is the map of film thickness, and  $\lambda$  is the attenuation length for photoelectrons from the substrate in the overlayer. For Si 2p electrons generated by Al K $\alpha$  X-rays attenuated in an average polymer, Eqn (8) results in an EAL of 3.83 nm. The film thickness map calculated using the

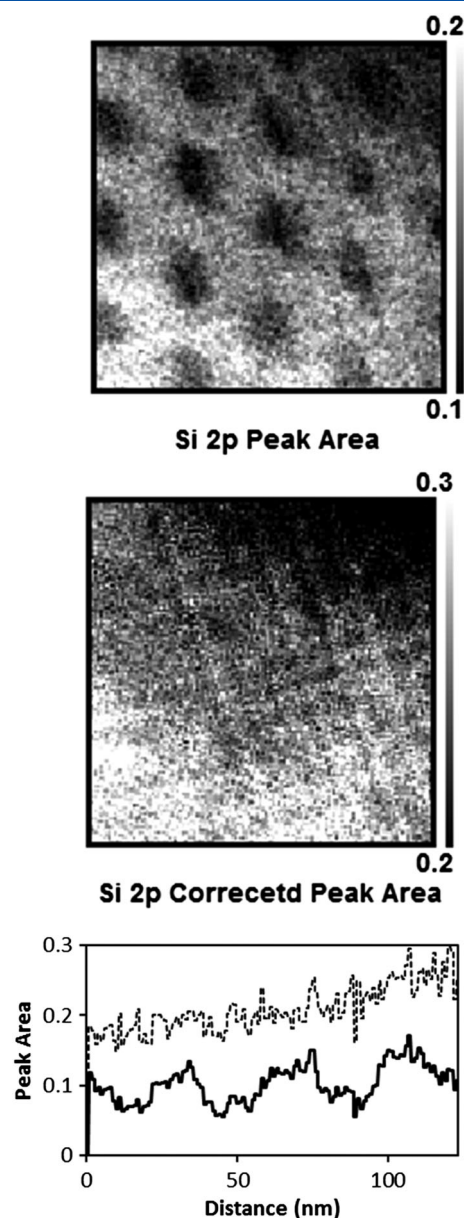


**Figure 10.** Si 2p photoelectron peak area image (top) and peak area image corrected for attenuation in the overlayer (lower), together with cross section along the indicated line from the uncorrected image (solid) and the corrected image (dashed). Eight hundred micrometre field of view.

Tougaard non-interactive method was used to correct the silicon photoelectron peak area image and the uncorrected and corrected images are shown in Fig. 10 displayed over the same range, together with a cross section along the ppHex islands. In the corrected image the decrease in intensity associated with the ppHex islands has been minimised and the remaining contrast is because of uneven X-ray illumination and striations from the delay line detector.

### Conclusions

The thickness of ppHex thin films deposited onto fused silica has been measured using ellipsometry and XPS to distinguish the effectiveness of different XP methods for both spectroscopy and



imaging. The universal equations, (7) and (8), were used to calculate the IMFP and EAL used in the calculations. Film thickness measurement using the OA method by quantification was the easiest method to implement but requires acquiring data for all elements present, whilst the OA method with the use of a bulk reference only requires acquiring data for the overlayer element. However both OA methods were sensitive to the changes in chemistry produced by the remnants of an oxygen plasma during the initial stages of deposition. For the thicker films, which had negligible oxidation, the bulk polymer reference produced thickness values within the estimated accuracy. This procedure therefore requires prior knowledge of the overlayer chemistry to enable selection of an appropriate bulk reference. The OA method by quantification also showed discrepancies for thick films, which arise because of errors associated with measuring low substrate intensities, particularly for elements with low sensitivity, propagating to all elements during the normalisation procedure.

Comparison of the thickness obtained using peak shape analysis and ellipsometry showed very good agreement up to 16 nm, provided that the appropriate scattering cross section was used, and did not appear to be sensitive to changes in the chemistry of the films. The procedure requires measurement around the C 1s photoelectron region, together with measurement of a bulk reference. Thickness values calculated using QUASES-Tougaard and Tougaard non-interactive methods showed slopes of 0.97 and 0.98 with values obtained from ellipsometry, well within the estimated accuracy.

Film thickness maps of the patterned ppHex films were successfully produced using both peak shape analysis and by measuring photoelectron peak areas. The thickness values produced were in agreement with the spectroscopic analysis where differences between the peak shape analysis methods and those using the photoelectron peak area for the thinner films were shown to arise due to interaction of the ppHex film with oxygen during initial deposition. Inspection of the C 1s spectrum summed from locations away from the ppHex islands showed that the polymer cross section is appropriate to describe inelastic scattering in the contamination overlayer, which allows use of a hydrocarbon polymer as a bulk reference for the contamination overlayer. The C 1s thickness map calculated using the Tougaard non-interactive method was successfully used to correct the intensity of the Si 2p peak area image for attenuation in the overlayer following determination of the EAL of silicon photoelectrons in the ppHex using the universal equation.

## References

- [1] H. Iwai, J. S. Hammond, S. Tanuma, *J. Surf. Anal.* **2009**, *15*, 264.
- [2] J. Walton, N. Fairley, *Surf. Interface Anal.* **2004**, *36*, 89. DOI:10.1002/sia.1654.
- [3] E. F. Smith, D. Briggs, N. Fairley, *Surf. Interface Anal.* **2006**, *38*, 69. DOI:10.1002/sia.2199.
- [4] F. De la Pena, N. Barrett, L. F. Zagonel, M. Walls, O. Renault, *Surf. Sci.* **2010**, *604*, 1628. DOI:10.1016/j.susc.2010.06.006.
- [5] B. P. Payne, A. P. Grosvenor, M. C. Biesinger, B. A. Kobe, N. S. McIntyre, *Surf. Interface Anal.* **2007**, *39*, 582. DOI:10.1002/sia.2565.
- [6] S. Hajati, S. Coultas, C. Blomfield, S. Tougaard, *Surf. Sci.* **2006**, *600*, 3015. DOI:10.1016/j.susc.2006.05.020.
- [7] S. Hajati, S. Tougaard, J. Walton, N. Fairley, *Surf. Sci.* **2008**, *602*, 3064. DOI:10.1016/j.susc.2008.08.005.
- [8] S. Tougaard, *J. Electron Spectrosc. Rel. Phenom.* **2010**, *178–179*, 128. DOI:10.1016/j.elspec.2009.08.005.
- [9] S. Hajati, S. Tougaard, *Anal. Bioanal. Chem.* **2010**, *396*, 2741. DOI:10.1007/s00216-009-3401-9.
- [10] M. P. Seah, R. White, *Surf. Interface Anal.* **2002**, *33*, 960. DOI:10.1002/sia.1478.
- [11] M. P. Seah, S. J. Spencer, *J. Vac. Sci. Technol. A* **2003**, *21*(2), 345. DOI:10.1116/1.1535173.
- [12] G. C. Smith, *J. Electron Spectrosc. Rel. Phenom.* **2005**, *148*, 21. DOI:10.1016/j.elspec.2005.02.004.
- [13] S. Tougaard, *Surf. Interface Anal.* **1998**, *26*, 249. DOI:10.1002/(SICI)1096-9918(199804)26:4<249::AID-SIA368>3.0.CO;2-A.
- [14] S. Tanuma, C. J. Powell, D. R. Penn, *Surf. Interface Anal.* **1994**, *21*, 165. DOI:10.1002/sia.740210302.
- [15] S. Tougaard, *J. Vac. Sci. Technol. A* **2003**, *21*(4), 1081. DOI:10.1116/1.1564040.
- [16] S. Tougaard, *J. Vac. Sci. Technol. A* **2005**, *23*(4), 741. DOI:10.1116/1.1864053.
- [17] S. Tougaard, *J. Vac. Sci. Technol. A* **2013**, *31*(3), 1. DOI:10.1116/1.4795246.
- [18] P. J. Cumpson, M. P. Seah, *Surf. Interface Anal.* **1997**, *25*, 430. DOI:10.1002/(SICI)1096-9918(199706)25:6<430::AID-SIA254>3.0.CO;2-7.
- [19] S. Tougaard, A. Jablonski, *Surf. Interface Anal.* **1997**, *25*, 404. DOI:10.1002/(SICI)1096-9918(199706)25:6<404::AID-SIA250>3.0.CO;2-A.
- [20] M. P. Seah, S. J. Spencer, *Surf. Interface Anal.* **2011**, *43*, 744. DOI:10.1002/sia.3607.
- [21] M. P. Seah, *Surf. Interface Anal.* **2012**, *44*, 497. DOI:10.1002/sia.4816.
- [22] M. P. Seah, *Surf. Interface Anal.* **2012**, *44*, 1353. DOI:10.1002/sia.5033.
- [23] S. A. Voronin, J. W. Bradley, C. Fotea, M. Zelzer, M. A. Alexander, *J. Vac. Sci. Technol. A* **2007**, *25*, 1093. DOI:10.1116/1.2712186.
- [24] J. Wernecke, A. G. Shard, N. Krumney, *Surf. Interface Anal.* **2014**, *46*, 911. DOI:10.1002/sia.5371.
- [25] M. P. Seah, S. J. Spencer, *Surf. Interface Anal.* **2009**, *41*, 960. DOI:10.1002/sia.3127.
- [26] J. H. Scofield, *J. Electron Spectrosc. Rel. Phenom.* **1976**, *8*, 129. DOI:10.1016/0368-2048(76)80015-1.
- [27] J. Walton, N. Fairley, *J. Electron Spectrosc. Rel. Phenom.* **2006**, *150*, 15. DOI:10.1016/j.elspec.2005.08.001.
- [28] M. P. Seah, *J. Electron Spectrosc. Relat. Phenom.* **1995**, *71*, 191. DOI:10.1016/0368-2048(94)02275-5.
- [29] A. S. Lea, K. R. Swanson, J. N. Haack, J. E. Castle, S. Tougaard, D. R. Baer, *Surf. Interface Anal.* **2010**, *42*, 1061. DOI:10.1002/sia.3304.